IJRCS

International Journal of Robotics and Control Systems
Vol. 4, No. 3, 2024, pp. 1490-1505
ISSN 2775-2658
http://pubs2.ascee.org/index.php/ijrcs

ASCEE

Control of a Multimode Double-Pendulum Overhead Crane System Using Input Shaping Controllers

Sharifah Yuslinda Syed Hussien [a,1], Hazriq Izzuan Jaafar [a,b,2,*], Rozaimi Ghazali [a,b,3], Liyana Ramli [c,4], Mohd Khairul Azizat Johari [d,5]

[a] Faculty of Electrical Technology and Engineering, Universiti Teknikal Malaysia Melaka, Hang Tuah Jaya, 76100 Durian Tunggal, Melaka, Malaysia
[b] Center for Robotics and Industrial Automation, Universiti Teknikal Malaysia Melaka, Hang Tuah Jaya, 76100 Durian Tunggal, Melaka, Malaysia
[c] Faculty of Engineering and Built Environment, Universiti Sains Islam Malaysia, 71800 Nilai, Negeri Sembilan, Malaysia
[d] Facility Development Department, Johor Port Berhad, 81707 Pasir Gudang, Johor, Malaysia
[1] sharifah.yuslinda@gmail.com; [2] hazriq@utem.edu.my; [3] rozaimi.ghazali@utem.edu.my; [4] lyanaramli@usim.edu.my; [5] azizat@johorport.com.my
* Corresponding Author

ARTICLE INFO

Article history
Received July 15, 2024
Revised August 26, 2024
Accepted August 29, 2024

Keywords
Double-Pendulum;
Input Shaping Controllers;
Multimode;
Oscillation Reduction;
Overhead Crane;
Payload Hoisting

ABSTRACT

This paper investigates the impact of higher derivative input shaping for minimizing both oscillations, namely hook and payload of a multimode double-pendulum overhead crane (MDPOC) system. The MDPOC has greater nonlinearities and stronger internal couplings, especially when involving two oscillation frequencies with multimode dynamic effects. With a suitable system's natural frequency and damping ratio of the hook and payload oscillations, multimode zero-vibration (ZV-ZV), multimode zero-vibration derivative (ZVD-ZVD) and multimode zero-vibration derivative-derivative (ZVDD-ZVDD) shapers are successfully designed. More interestingly, two scenarios under a fixed cable length and a payload hoisting are considered which are closer to the real practical crane. Thus, an average travel length (ATL)-based shaper method is also considered to further verify the effectiveness and robustness of efficient hook and payload oscillation control under payload hoisting. All the multimode input shaping is simulated using the Matlab software. The simulation results of multimode ZVDD-ZVDD shaper successfully reduced in the overall hook and payload oscillations by 97.9% and 97.2%, respectively, compared to the unshaped system, whereas the multimode ATL-ZVDD shaper reduced hook and payload oscillations by 94.8% and 94.0%, respectively. In fact, the multimode ZVDD-ZVDD and multimode ATL-ZVDD shapers demonstrate the superiority in minimizing the hook and payload oscillations compared to the multimode ZV-ZV, multimode ZVD-ZVD, ATL-ZV and ATL-ZVD shapers. This significant reduction in oscillations enhances the precision and safety of real-world crane operations in industrial settings. It has been proven that considering the additional derivative of input shaping results in a higher level of hook and payload oscillations reduction.

This is an open-access article under the CC–BY-SA license.

1. Introduction

The input shaping approach is one of the most common control strategies for real-time applications such as robotics, flexible structures and other control systems that involve vibration/oscillations motion [1]-[8]. Singer and Seering made the first proposal for input shaping [9]. A command input signal is convolved with a sequence of impulses at different points to reduce the oscillation of the system. The shaper consists of impulses with magnitudes and time locations based on the system's natural frequency and damping ratio [10]. The second impulse will cancel out the oscillation induced by the first impulse if the impulse sequence is applied with the required amplitudes. Therefore, the full response of a shaped signal can be acquired, as illustrated in Fig. 1. With an understanding of the shaped generation concept, many researchers have expressed interest in the input shaping method [11]-[16] and crane system is chosen as a suitable industrial application for this study [17]-[22].

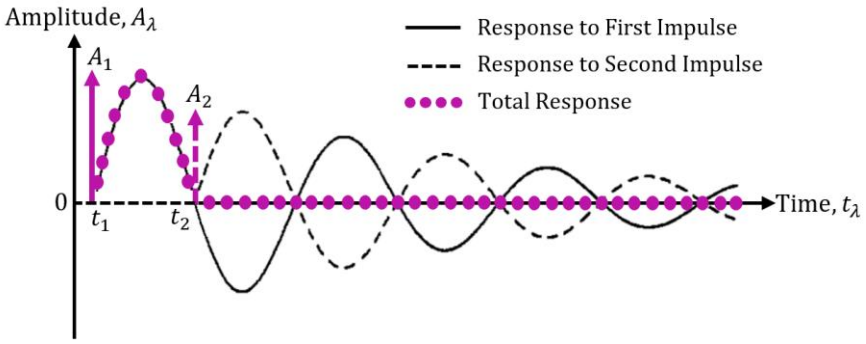

Fig. 1. Shaped generation concept of input shaping

Most input shaping techniques have been focused on single-pendulum overhead crane (SPOC) systems [23]-[29]. However, single-mode oscillation-based input shaping techniques are inappropriate for application in double-pendulum overhead crane (DPOC) system, which have two separate frequency modes (hook and payload) [30]-[35]. The SPOC makes certain assumptions, including without accounting for a hook or an extra sling cable. In addition, the hook and payload are essentially combined and treated as a single mass point to reduce the complexity of the crane model [36]-[45]. This has the potential to degrade the input shaping control's effectiveness and robustness. Therefore, some modifications to input shaping are required to reduce overall system oscillation. As a solution, Singhose et al. proposed a strategy through convolution of several single-mode input shaping, which was successfully applied to a DPOC [46]. To create a two-mode input shaping, additional information regarding the system's natural frequency and damping ratio was necessary, which target both the first and second modes of oscillations.

Kenison and Singhose extended their research into two-mode input shaping by proposing a two-mode specified insensitivity (SI) to eliminate hook and payload oscillations. Experimental studies demonstrated the usefulness of the shaper in terms of efficiency and safety [47]. As opposed to manual control, crane operators' work completion times were much faster, and operator effort was greatly reduced. In addition, a two-mode zero-vibration (ZV) input shaping has been introduced by Manning et al. and Vaughan et al. [48]. A significant number of crane operators have demonstrated a thorough study of the two-mode ZV when operating DPOC systems. Therefore, the two-mode ZV shaper allowed the operators to maneuver the trolley with low oscillations. Furthermore, the shaper was evaluated under various payload masses, and the experimental findings showed that the two-mode ZV shaper reduced oscillations more effectively than the proportional-derivative (PD) controller.

In addition, a ZV derivative (ZVD) shaper has also been developed to improve the input shaping robustness for a DPOC [49]-[50]. The ZVD shaper relies heavily on the estimated system's natural frequency and damping ratio. The purpose is to generate three sets of impulse sequences, as opposed to the ZV design, which requires two sets of impulses. In fact, the principal ZVD shaper has been used

for developing the frequency-modulation input shaping [46], [51]. Interestingly, the testing results demonstrated that an extra derivative in the ZVD shaper provided a higher level of oscillation reduction and robustness towards system's parameter adjustments. Due to the additional third impulse, the ZVD shaper's robustness unfortunately caused a longer (slower) trolley position response time.

Furthermore, a ZV derivative-derivative (ZVDD) shaper is a sophisticated control approach to reduce residual oscillation in DPOC systems. It expands on the concept of ZVD shapers by incorporating both velocity and acceleration (second derivative) elements from the input signal. This technique aims to further suppress vibrations by addressing the system's higher-order dynamics. This approach has various advantages, including increased vibration control and greater control over system dynamics. By incorporating derivative terms, the input shaper may more effectively counteract the displacement and velocity components of the system's response, resulting in improved oscillation and vibration suppression [17].

In this study, three types of multimode input shaping controllers are investigated for a multimode DPOC (MDPOC) system. Simulations with a dynamic model were conducted under two conditions: (1) Fixed cable length and (2) Payload hoisting, which are closer to the actual operational crane. In summary, the contributions of this paper can be listed as follows:

1) Input shaping controllers with respective natural frequency and damping ratio are proposed to minimize the hook and payload oscillations of MDPOC.
2) The additional derivative of input shaping controllers provided a higher level of hook and payload oscillation reduction.
3) The average travel length (ATL) with higher derivative of input shaping controllers offers benefits such as higher level of hook and payload oscillations reduction under payload hoisting.

2. Multimode DPOC (MDPOC)

In this section, a fixed cable length and a payload hoisting (varying cable length) are considered in minimizing the hook and payload oscillations of the MDPOC as illustrated in Fig. 2. The MDPOC consists of four independent generalized coordinates (trolley position, x, hook angle, θ_1, payload angle, θ_2, and cable length, l_1). The trolley mass, the hook mass, the payload mass, the fixed/varying cable length, the sling cable, the trolley viscous damping coefficient and the gravitational acceleration constant, represent m, m_1, m_2, l_1, l_2, f_x and g, respectively. F_x and F_l are the two external forces that is applied directly to the MDPOC as the trolley and hoisting input signals.

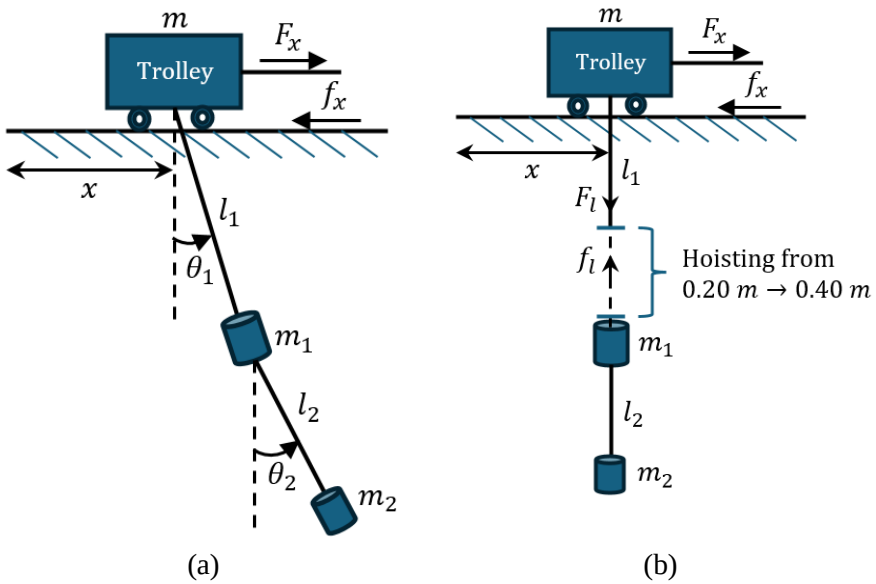

Fig. 2. Illustration of MDPOC: (a) A fixed cable length (b) A payload hoisting

With a fixed cable length, the MDPOC dynamic equations can be expressed as [17]:

$$(m+m_1+m_2)\ddot{x} + (m_1+m_2)l_1\ddot{\theta}_1\,\mathrm{c}(\theta_1) + m_2l_2\ddot{\theta}_2\,\mathrm{c}(\theta_2) - (m_1+m_2)l_1\dot{\theta}_1{}^2\,\mathrm{s}(\theta_1) - m_2l_2\dot{\theta}_2{}^2\,\mathrm{s}(\theta_2) = F_x - f_x\dot{x} \tag{1}$$

$$(m_1+m_2)l_1\ddot{x}\,\mathrm{c}(\theta_1) + (m_1+m_2)l_1{}^2\ddot{\theta}_1 + m_2l_1l_2\ddot{\theta}_2\,\mathrm{c}(\theta_1-\theta_2) + m_2l_1l_2\dot{\theta}_2{}^2\,\mathrm{s}(\theta_1-\theta_2) + (m_1+m_2)gl_1\,\mathrm{s}(\theta_1) = 0 \tag{2}$$

$$m_2l_2\ddot{x}\,\mathrm{c}(\theta_2) + m_2l_1l_2\ddot{\theta}_1\,\mathrm{c}(\theta_1-\theta_2) + m_2l_2{}^2\ddot{\theta}_2 - m_2l_1l_2\dot{\theta}_1{}^2\,\mathrm{s}(\theta_1-\theta_2) + m_2gl_2\,\mathrm{s}(\theta_2) = 0 \tag{3}$$

where s and c represent sin and cos, respectively.

In industrial practice, the l_1 changes during payload hoisting, which involves lifting a payload up or down and transfer it at a specific location, as seen in Fig. 2 (b). Therefore, F_l is needed as an external hoisting force signal for varying cable length and f_l denotes the viscous damping coefficients of l_1. Thus, the MDPOC with payload hoisting can be obtained as in (4)-(7) [17], [30].

$$(m+m_1+m_2)\ddot{x} + (m_1+m_2)[2\dot{l}_1\dot{\theta}_1\,\mathrm{c}(\theta_1) + l_1\ddot{\theta}_1\,\mathrm{c}(\theta_1) - l_1\dot{\theta}_1{}^2\,\mathrm{s}(\theta_1) + \ddot{l}_1\,\mathrm{s}(\theta_1)] + m_2l_2[\ddot{\theta}_2\,\mathrm{c}(\theta_2) - \dot{\theta}_2{}^2\,\mathrm{s}(\theta_2)] = F_x - f_x\dot{x} \tag{4}$$

$$(m_1+m_2)[\ddot{x}l_1\,\mathrm{c}(\theta_1) + l_1{}^2\ddot{\theta}_1 + gl_1\,\mathrm{s}(\theta_1) + 2l_1\dot{l}_1\dot{\theta}_1] + m_2l_1l_2[\ddot{\theta}_2\,\mathrm{c}(\theta_1-\theta_2) + \dot{\theta}_2{}^2\,\mathrm{s}(\theta_1-\theta_2)] = 0 \tag{5}$$

$$m_2l_2[\ddot{x}\,\mathrm{c}(\theta_2) + l_2\ddot{\theta}_2 + \ddot{l}_1\,\mathrm{s}(\theta_1-\theta_2) - l_1\dot{\theta}_1{}^2\,\mathrm{s}(\theta_1-\theta_2) + l_1\ddot{\theta}_1\,\mathrm{c}(\theta_1-\theta_2) + 2\dot{l}_1\dot{\theta}_1\,\mathrm{c}(\theta_1-\theta_2) + g\,\mathrm{s}(\theta_2)] = 0 \tag{6}$$

$$(m_1+m_2)[\ddot{x}\,\mathrm{s}(\theta_1) + \ddot{l}_1 - l_1\dot{\theta}_1{}^2 + g(1-\mathrm{c}(\theta_1))] + m_2l_2[\ddot{\theta}_2\,\mathrm{s}(\theta_1-\theta_2) - \dot{\theta}_2{}^2\,\mathrm{c}(\theta_1-\theta_2)] = F_l - f_l\dot{l}_1 \tag{7}$$

Therefore, the control challenge is to obtain low hook and payload oscillations angle of θ_1 and θ_2 respectively during trolley transportation. The simulations' system parameters, which match the INTECO crane model are shown in Table 1 [30].

3. Multimode Input Shaping Controllers

This section describes and formulates the multimode input shaping controllers as feedforward control designs. The aim of input shaping is to modify the original command signal, thus reducing hook and payload oscillations. This includes ATL-based shaper methods to further verify the robustness of efficient hook and payload oscillation control under payload hoisting [46], [52]-[60].

3.1. Multimode ZV-ZV Shaper

A set of impulses called input shaping are created depending on the system's natural frequency, ω_n and damping ratio, ζ [17]. The residual vibration, v that results from convolving an input signal with a sequence of impulses is given as:

$$v(\omega_n,\zeta) = e^{-\zeta\omega_n t_\lambda}\sqrt{c(\omega_n,\zeta)^2 + s(\omega_n,\zeta)^2} \tag{8}$$

where:

$$c(\omega_n, \zeta) = \sum_{\lambda=1}^{M} A_\lambda \, e^{-\zeta \omega_n t_\lambda} \, \mathrm{c}(\omega_d t_\lambda) \tag{9}$$

$$s(\omega_n, \zeta) = \sum_{\lambda=1}^{M} A_\lambda \, e^{-\zeta \omega_n t_\lambda} \, \mathrm{s}(\omega_d t_\lambda) \tag{10}$$

The positive amplitudes and time locations of the impulse series are denoted as A_λ and t_λ, respectively. To maintain the same output magnitude, the total of the A_λ is set to unity as follow:

$$\sum_{\lambda=1}^{M} A_\lambda = 1 \tag{11}$$

where M denotes the maximum number of impulses. By solving (8)-(11), in which $v(\omega_n, \zeta)$ equals zero, the ZV shaper can be designed with A_λ and t_λ of a two-impulse shaper ($M = 2$) as follows:

$$\begin{bmatrix} A_\lambda \\ t_\lambda \end{bmatrix} = \begin{bmatrix} A_1 & A_2 \\ t_1 & t_2 \end{bmatrix} \tag{12}$$

$$A_1 = \frac{1}{1+H}; \; A_2 = \frac{H}{1+H}; \; t_1 = 0 \text{ and } t_2 = \frac{\pi}{\omega_d} \tag{13}$$

where $\omega_d = \omega_n \sqrt{1-\zeta^2}$ and $H = e^{-\frac{\zeta\pi}{\sqrt{1-\zeta^2}}}$. Fig. 3 depicts the convolution process of ZV shaper.

Table 1. MDPOC parameters

Variables	Parameters		
	Symbol	Values	Unit
Trolley Mass	m	1.155	kg
Hook Mass	m_1	0.20	kg
Payload Mass	m_2	0.10	kg
Fixed Cable Length and Payload Hoisting	l_1	0.30 and 0.20 – 0.40	m
Sling Cable	l_2	0.20	m
Trolley Viscous Damping Coefficient	f_x	82	Ns/m
Hoisting Viscous Damping Coefficient	f_l	75	Ns/m
Gravitational Constant	g	9.81	m/s^2

To eliminate undesirable hook and payload oscillations, an MDPOC system requires the convolution of two ZV shapers, called as a multimode ZV-ZV shaper. Thus, it is necessary to obtain the value of ω_n and ζ for each mode of both oscillations. In this work, the curve fitting toolbox [49] was used to estimate the ω_n and ζ values of MDPOC. After carefully determining the cable lengths $l_1 = 0.30$ m and $l_2 = 0.20$ m, the values of ω_n and ζ values for modes 1 and 2 were determined to be 5.226 rad/s and 0.01334, and 9.872 rad/s and 0.05183, respectively. The ZV shaper parameters for every mode were then generated by solving (12) and (13). Subsequently, (14) and (15) were convolved together to form a multimode ZV-ZV shaper for handling both oscillations.

$$\begin{bmatrix} A_{ZV} \\ t_{ZV} \end{bmatrix} = \begin{bmatrix} 0.5105 & 0.4895 \\ 0 & 0.6013 \end{bmatrix} \quad \text{(Mode 1)} \tag{14}$$

$$\begin{bmatrix} A_{ZV} \\ t_{ZV} \end{bmatrix} = \begin{bmatrix} 0.5407 & 0.4593 \\ 0 & 0.3187 \end{bmatrix} \quad \text{(Mode 2)} \tag{15}$$

3.2. Multimode ZVD-ZVD Shaper

A ZVD shaper is a three-impulse shaper ($M = 3$) that is intended to boost shaper robustness. Fig. 4 depicts the ZVD input shaper, which can be created using the convolution process as:

$$\begin{bmatrix} A_\lambda \\ t_\lambda \end{bmatrix} = \begin{bmatrix} A_1 & A_2 & A_3 \\ t_1 & t_2 & t_3 \end{bmatrix} \tag{16}$$

$$A_1 = \frac{1}{(1+H)^2}; A_2 = \frac{2H}{(1+H)^2};\ A_3 = \frac{H^2}{(1+H)^2}; \tag{17}$$

$$t_1 = 0;\ t_2 = \frac{\pi}{\omega_d} \text{ and } t_3 = \frac{2\pi}{\omega_d} \tag{18}$$

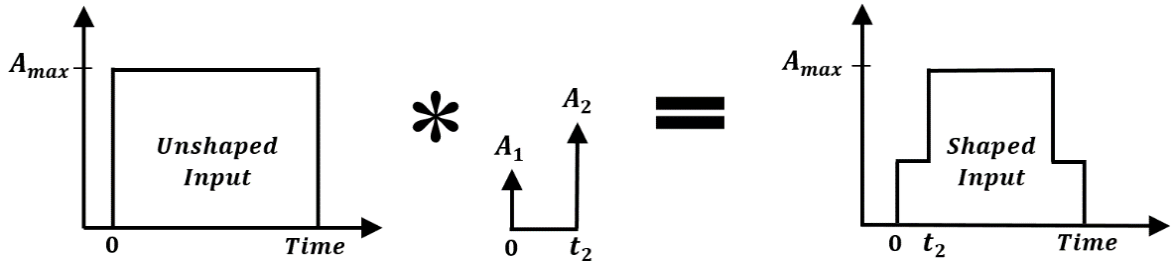

Fig. 3. Illustration of ZV shaper convolution

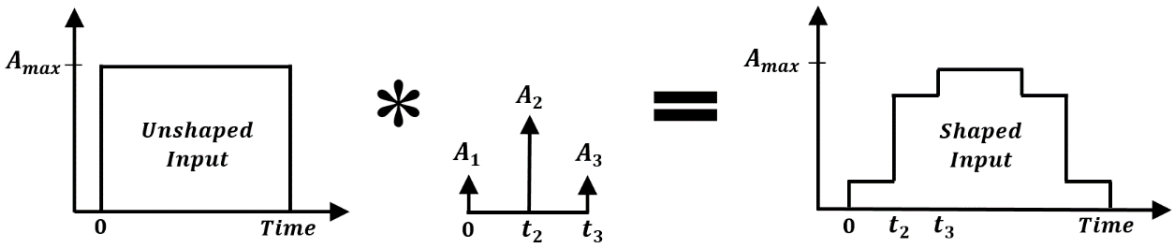

Fig. 4. Illustration of ZVD shaper convolution

Similar values of ω_n and ζ were used to calculate the ZVD shaper for each mode by solving (16) to (18) separately, resulting in ZVD shaper parameters as in (19) and (20). Subsequently, (19) and (20) were convolved together to develop multimode ZVD-ZVD shaper.

$$\begin{bmatrix} A_{ZVD} \\ t_{ZVD} \end{bmatrix} = \begin{bmatrix} 0.2606 & 0.4998 & 0.2396 \\ 0 & 0.6013 & 1.2026 \end{bmatrix} \quad \text{(Mode 1)} \tag{19}$$

$$\begin{bmatrix} A_{ZVD} \\ t_{ZVD} \end{bmatrix} = \begin{bmatrix} 0.2923 & 0.4967 & 0.2110 \\ 0 & 0.3187 & 0.6374 \end{bmatrix} \quad \text{(Mode 2)} \tag{20}$$

3.3. Multimode ZVDD-ZVDD Shaper

With four-impulse shaper ($M = 4$), ZVDD is designed to further increase the shaper robustness as shown in Fig. 5. Through the convolution process, the ZVDD shaper can be formulated as:

$$\begin{bmatrix} A_\lambda \\ t_\lambda \end{bmatrix} = \begin{bmatrix} A_1 & A_2 & A_3 & A_4 \\ t_1 & t_2 & t_3 & t_4 \end{bmatrix} \tag{21}$$

$$A_1 = \frac{1}{(1+H)^3}; A_2 = \frac{3H}{(1+H)^3};\ A_3 = \frac{3H^2}{(1+H)^3};\ A_4 = \frac{H^3}{(1+H)^3} \tag{22}$$

$$t_1 = 0;\ t_2 = \frac{\pi}{\omega_d};\ t_3 = \frac{2\pi}{\omega_d}; \text{and } t_4 = \frac{3\pi}{\omega_d} \tag{23}$$

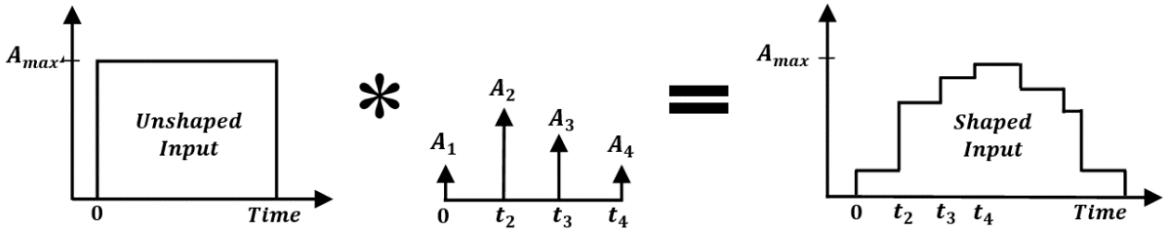

Fig. 5. Illustration of ZVDD shaper convolution

Similarly, (24) and (25) were convolved together to yield multimode ZVDD-ZVDD shaper.

$$\begin{bmatrix} A_{ZVDD} \\ t_{ZVDD} \end{bmatrix} = \begin{bmatrix} 0.1330 & 0.3827 & 0.3670 & 0.1173 \\ 0 & 0.6012 & 1.2024 & 1.8036 \end{bmatrix} \quad \text{(Mode 1)} \tag{24}$$

$$\begin{bmatrix} A_{ZVDD} \\ t_{ZVDD} \end{bmatrix} = \begin{bmatrix} 0.1581 & 0.4028 & 0.3422 & 0.0969 \\ 0 & 0.3187 & 0.6373 & 0.9560 \end{bmatrix} \quad \text{(Mode 2)} \tag{25}$$

3.4. Multimode ATL-ZV, Multimode ATL-ZVD and Multimode ATL-ZVDD Shapers

During payload hoisting operation, ω_n and ζ fluctuate significantly and can be designed via ATL approach [56]-[57]. Hence, the multimode ZV-ZV, multimode ZVD-ZVD and multimode ZVDD-ZVDD shapers designed with $l_1 = 0.30$ m in Sections 3.1, 3.2 and 3.3 respectively are also the ATL-based shapers. Therefore, multimode ATL-ZV, multimode ATL-ZVD and multimode ATL-ZVDD shapers are expected to perform effectively under payload hoisting conditions. This allows for a fair comparison of the three ATL-based shapers.

4. Results and Discussion

Two simulation scenarios: (1) Fixed cable length and (2) Payload hoisting are presented in this section. The designed multimode ZV-ZV, multimode ZVD-ZVD and multimode ZVDD-ZVDD shapers were tested under fixed cable length conditions, while multimode ATL-ZV, multimode ATL-ZVD and multimode ATL-ZVDD shapers were executed under payload hoisting conditions. All the multimode input shaping was applied to the MDPOC model as shown in Fig. 6.

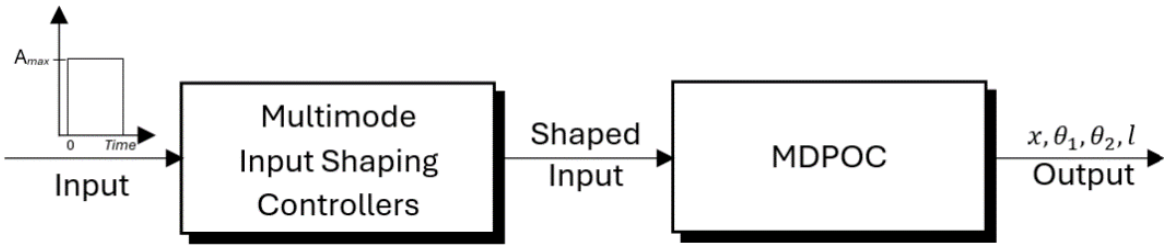

Fig. 6. A block diagram with multimode input shaping controllers

An external input force as plotted in Fig. 7 was stimulated into the multimode input shaping controllers (multimode ZV-ZV, multimode ZVD-ZVD and multimode ZVDD-ZVDD) and converted as shaped input to maneuver the MDPOC as illustrated in Fig. 8.

In this work, the maximum amplitude of hook, θ_{1m} and payload, θ_{2m} angles was measured. Furthermore, a performance indicator known as mean squared error of hook, MSE_{θ_1} and payload, MSE_{θ_2} was also used. Low values of θ_{1m}, θ_{2m}, MSE_{θ_1} and MSE_{θ_2} indicate minimal oscillations,

which are critical for ensuring the stability and precision of the MDPOC system in real-world operations. The most effective controller among the others is the one with the lowest θ_{1m}, θ_{2m}, MSE_{θ_1} and MSE_{θ_2}.

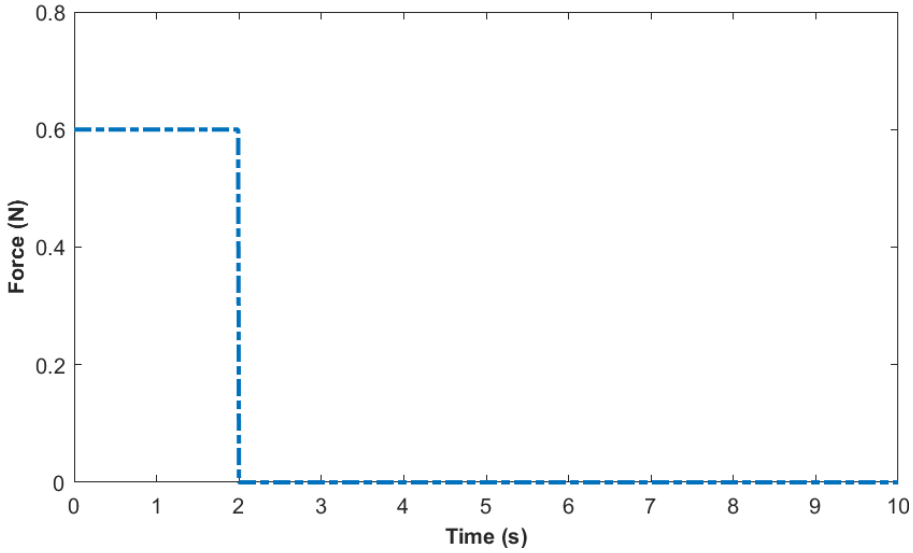

Fig. 7. An external force

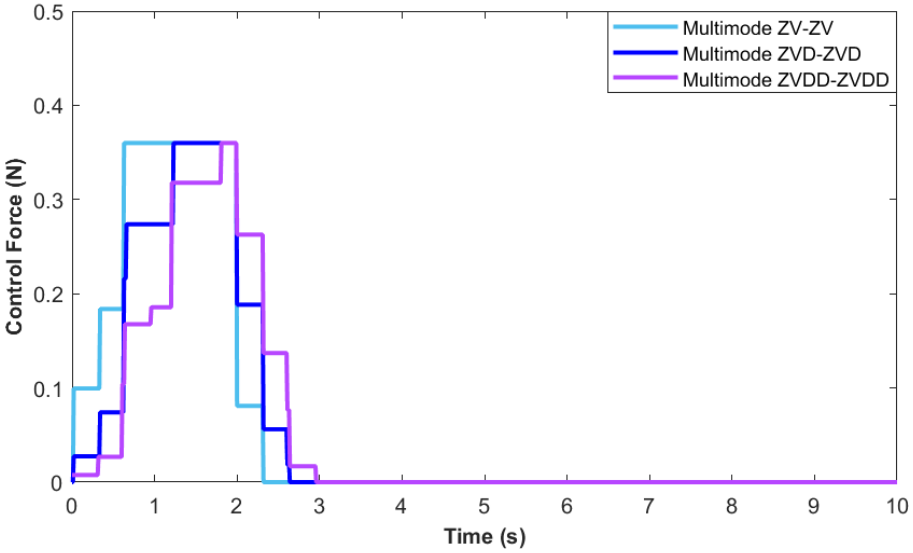

Fig. 8. Shaped control inputs

4.1. Fixed Cable Length

In this scenario, fixed cable lengths, $l_1 = 0.30$ m and $l_2 = 0.20$ m are investigated. Figs. 9, 10(a) and 10(b) depict the trolley position and both oscillations obtained with the multimode ZV-ZV, multimode ZVD-ZVD and multimode ZVDD-ZVDD. Fig. 10 summarizes the maximum and overall oscillations achieved using the controllers. In addition, Table 2 shows the performances of the multimode ZV-ZV, multimode ZVD-ZVD and multimode ZVD-ZVD shapers. The results indicate that multimode ZVDD-ZVDD provided the highest oscillations reduction. The multimode ZVDD-ZVDD provided 97.9%, 75.3% and 48.3% reductions in the overall hook oscillations and 97.2%, 67.6% and 38.5% reductions in the overall payload oscillations when compared to the unshaped, multimode ZV-ZV and multimode ZVD-ZVD shapers, respectively. As expected, the multimode ZVDD-ZVDD shaper reduced oscillations more effectively in all aspects than the multimode ZV-ZV and multimode ZVD-ZVD shapers.

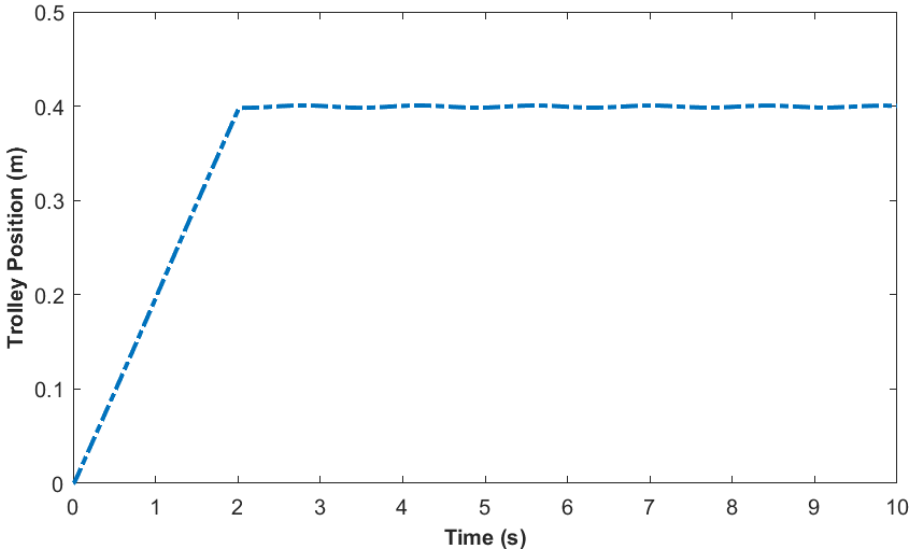

Fig. 9. Response of trolley position

4.2. Payload Hoisting

To investigate the efficiency of multimode input shaping, a payload hoisting scenario (from 0.20 m to 0.40 m) is also considered, as plotted in Fig. 11. During payload hoisting operation, ω_n and ζ fluctuate based on varying cable length. Therefore, the controller's robustness towards frequency fluctuations should be evaluated. As a result, Fig. 12 (a) and Fig. 12 (b) demonstrate the hook and payload oscillations, respectively. The maximum and overall oscillations are summarized in Fig. 12. Table 3 also shows the performances between unshaped and multimode ATL-based shapers.

Table 2. Performances of multimode shapers under a fixed cable length

Shapers	(a)	θ_{1m}	θ_{2m}	(b)	MSE_{θ_1}	MSE_{θ_2}
Unshaped		8.444^0	12.295^0		31.250	73.809
Multimode ZV-ZV		3.048^0	5.272^0		2.639	6.327
Multimode ZVD-ZVD		2.267^0	4.215^0		1.259	3.335
Multimode ZVDD-ZVDD		1.582^0	3.409^0		0.651	2.052

Similarly, the multimode ATL-ZVDD was demonstrated to have the highest robustness, particularly in controlling the hook and payload oscillations. The multimode ATL-ZVDD reduced overall hook oscillations by 94.8%, 60.9% and 35.5% compared to the unshaped, multimode ATL-ZV and multimode ATL-ZVD shapers, respectively, as well as overall payload oscillations by 94.0%, 52.6% and 26.6%. Thus, the multimode ATL-ZVDD shaper reduced oscillations more than the multimode ATL-ZV and multimode ATL-ZVD shapers, demonstrating its robustness and effectiveness in handling frequency fluctuations. Overall, the multimode ZVDD-ZVDD shaper proved to be the most effective for fixed cable lengths, while the multimode ATL-ZVDD shaper demonstrated superior performance during payload hoisting. However, the design and implementation of additional derivative shapers are typically more complex than standard input shapers. In addition, the multimode input shapers design is heavily reliant on the estimated system's ω_n and ζ for both hook and payload oscillations.

Table 3. Performances of multimode ATL-based shapers under a payload hoisting

Shapers	(c)	θ_{1m}	θ_{2m}	(d)	MSE_{θ_1}	MSE_{θ_2}
Unshaped		8.602^0	14.044^0		13.861	29.717
Multimode ATL-ZV		2.507^0	4.154^0		1.826	3.778
Multimode ATL-ZVD		1.956^0	3.471^0		1.107	2.442
Multimode ATL-ZVDD		1.482^0	3.120^0		0.714	1.792

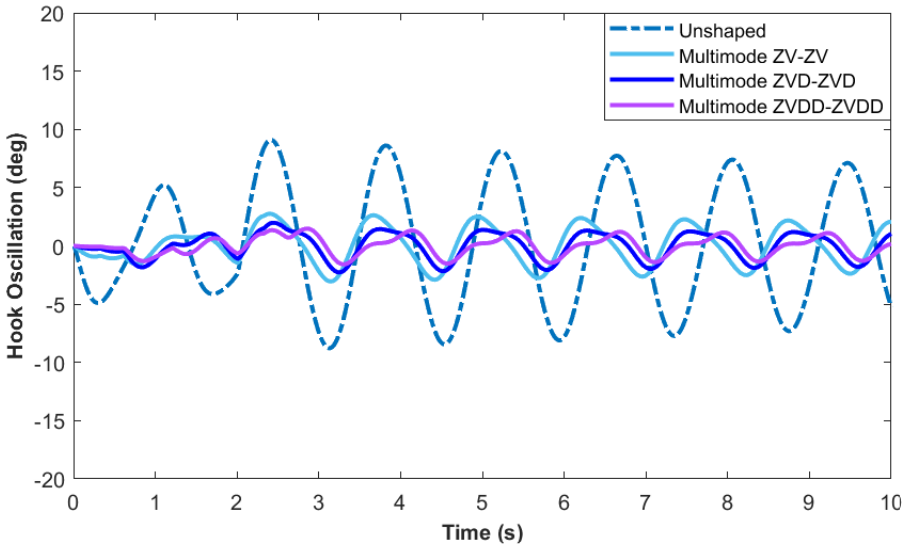

(a)

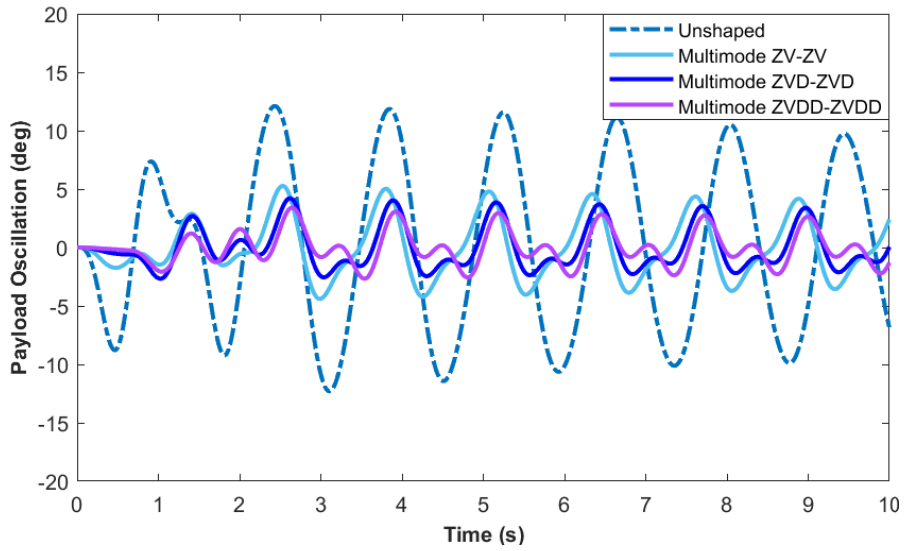

(b)

Fig. 10. Responses of oscillation with a fixed cable length: (a) Hook (b) Payload

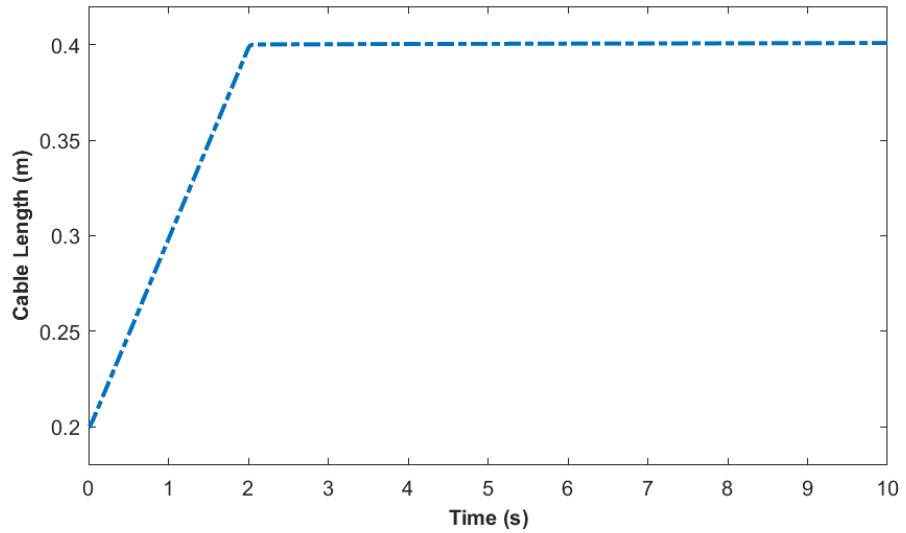

Fig. 11. Response of payload hoisting from 0.20 m to 0.40 m

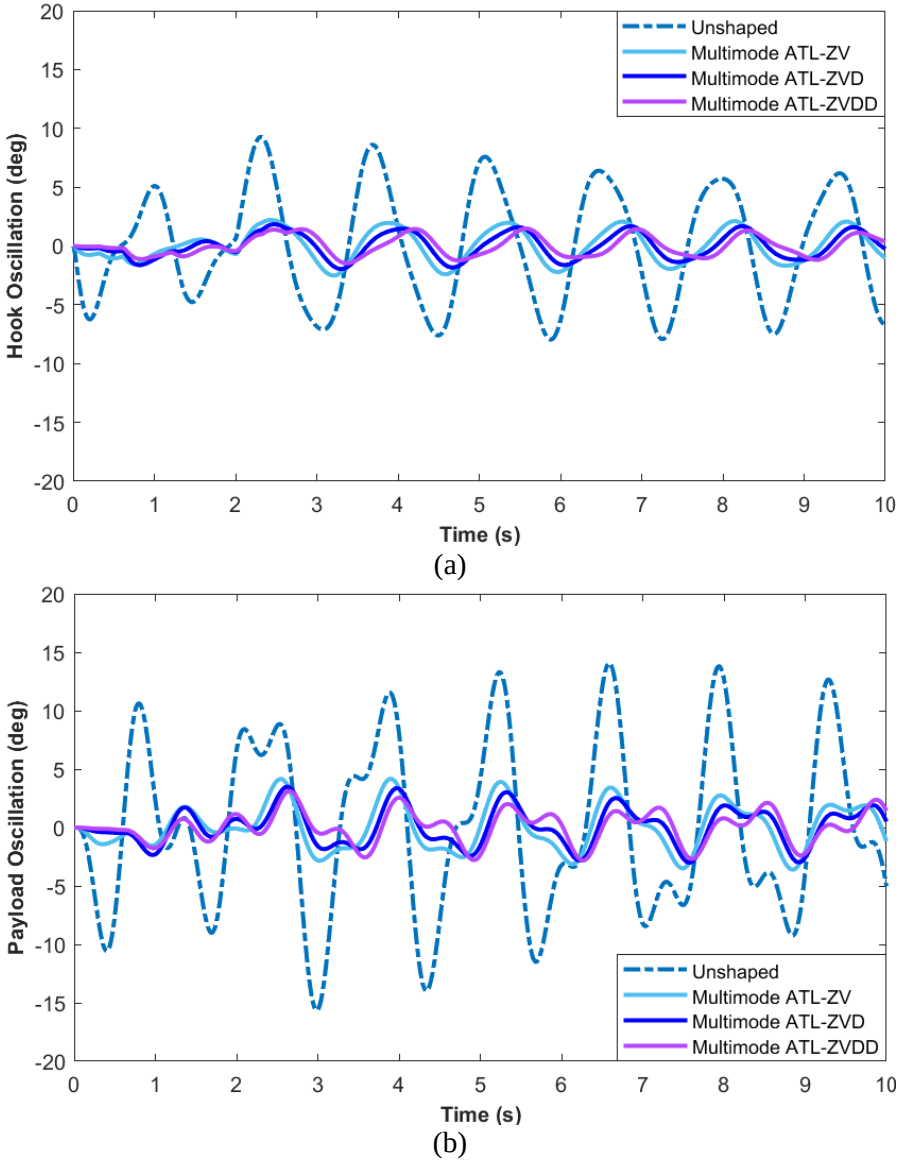

Fig. 12. Responses of oscillation with a payload hoisting: (a) Hook (b) Payload

5. Conclusion

A multimode input shaping controller provides an established feedforward control approach for minimizing hook and payload oscillations in an MDPOC system under fixed cable length and payload hoisting. The multimode ZVDD-ZVDD shaper successfully reduced in the overall hook and payload oscillations by 97.9% and 97.2%, respectively, compared to the unshaped system, whereas the multimode ATL-ZVDD shaper reduced hook and payload oscillations by 94.8% and 94.0%, respectively. Furthermore, the multimode ZVDD-ZVDD shaper has demonstrated the ability to achieve the highest reduction in both hook and payload oscillations when compared to the multimode ZV-ZV and multimode ZVD-ZVD shapers. In fact, the multimode ATL-ZVDD shaper was shown to be robust in modelling uncertainties related to variations in oscillation frequency during payload hoisting over the multimode ATL-ZV and multimode ATL-ZVD shapers. This significant reduction in oscillations enhances the precision and safety of real-world crane operations in industrial settings. However, the design and implementation of additional derivative shapers are typically more complex than standard input shapers. In addition, the multimode input shapers design is heavily reliant on the estimated system's ω_n and ζ for both hook and payload oscillations. Future research will explore

adaptive or learning-based multimode control strategies that dynamically adjust to system changes without the need for estimate ω_n and ζ.

Author Contribution: All authors contributed equally to the main contributor to this paper. All authors read and approved the final paper.

Funding: This research was funded by the Fundamental Research Grant Scheme (FRGS) and grant number FRGS/1/2021/TK0/UTEM/02/1.

Acknowledgment: The authors would like to thank the Ministry of Higher Education and Universiti Teknikal Malaysia Melaka (UTeM) for providing financial support under FRGS.

Conflicts of Interest: The authors declare no conflict of interest.

References

[1] D. K. Thomsen, R. S-Knudsen, O. Balling and X. Zhang, "Vibration Control of Industrial Robot Arms by Multi-Mode Time-Varying Input Shaping," *Mechanism and Machine Theory*, vol. 155, p. 104072, 2021, https://doi.org/10.1016/j.mechmachtheory.2020.104072.

[2] J. A. G. L. Junior, J. M. Balthazar, M. A. Ribeiro, F. C. Janzen and A. M. Tusset, "Dynamic Model of a Robotic Manipulator with One Degree of Freedom with Friction Component," *International Journal of Robotics and Control Systems*, vol. 3, no. 2, pp. 315-329, 2023, https://doi.org/10.31763/ijrcs.v3i2.984.

[3] B. Ataei, S. Yuan, Z. Ren and K. H. Halse, "Effects of Structural Flexibility on the Dynamic Responses of Low-Height Lifting Mechanism for Offshore Wind Turbine Installation," *Marine Structures*, vol. 89, p. 103399, 2023, https://doi.org/10.1016/j.marstruc.2023.103399.

[4] J. Haas, B. Schrage, G. Menze, P. M. Sieberg and D. Schramm, "Oscillation and Vibration Reduction Approaches on a HiL-Steering-Test-Bench," *IEEE/ASME Transactions on Mechatronics*, vol. 29, no. 2, pp. 1295-1305, 2024, https://doi.org/10.1109/TMECH.2023.3297949.

[5] Y. Wang, X. Li and Y. Shen, "Study on Mechanical Vibration Control of Limit Cycle Oscillations in the Van der Pol Oscillator by means of Nonlinear Energy Sink," *Journal of Vibration Engineering & Technologies*, vol. 12, pp. 811-819, 2024, https://doi.org/10.1007/s42417-023-00877-w.

[6] A. B. Alhassan, R. Chancharoen, B. B. Muhammad and G. Phanomchoeng, "Precise Automation of Rotary Flexible Link Manipulator Using Hybrid Input Shaping With Single State Feedback Fuzzy Logic and Sliding Mode Controllers," *IEEE Access*, vol. 11, pp. 86711-86726, 2023, https://doi.org/10.1109/ACCESS.2023.3304751.

[7] M. Elouni, H. Hamdi, B. Rabaoui and N. B. Braiek, "Adaptive PID Fault-Tolerant Tracking Controller for Takagi-Sugeno Fuzzy Systems with Actuator Faults: Application to Single-Link Flexible Joint Robot," *International Journal of Robotics and Control Systems*, vol. 2, no. 3, pp. 523-546, 2022, https://doi.org/10.31763/ijrcs.v2i3.762.

[8] Z. Guo, J. Zhang and P. Zhang, "Research on the Residual Vibration Suppression of Delta Robots Based on the Dual-Modal Input Shaping Method," *Actuators*, vol. 2, no. 3, p. 84, 2023, https://doi.org/10.3390/act12020084.

[9] C. Li, X. Huo and Q. Liu, "A New Robust Command Shaping Method and Its Application in Quadrotor Slung System with Varying Parameters," *IFAC-PapersOnLine*, vol. 53, no. 2, pp. 5737-5742, 2020, https://doi.org/10.1016/j.ifacol.2020.12.1603.

[10] H. Ghorbani, K. Alipour, B. Tarvirdizadeh and A. Hadi, "Comparison of Various Input Shaping Methods in Rest-to-Rest Motion of the End-Effecter of a Rigid-Flexible Robotic System with Large Deformations Capability," *Mechanical Systems and Signal Processing*, vol. 118, pp. 584-602, 2019, https://doi.org/10.1016/j.ymssp.2018.09.003.

[11] M. Newman, K. Lu and M. Khoshdarregi, "Suppression of Robot Vibrations using Input Shaping and Learning-based Structural Models," *Journal of Intelligent Material Systems and Structures*, vol. 32, no. 9, pp. 1001-1012, 2021, https://doi.org/10.1177/1045389X20947166.

[12] S. Baklouti, E. Courteille, P. Lemoine and S. Caro, "Input Shaping for Feed-Forward Control of Cable-Driven Parallel Robots," *Journal of Dynamic Systems, Measurement, and Control*, vol. 143, no. 2, p. 021007, 2021, https://doi.org/10.1115/1.4048354.

[13] A. Avazov, F. Colas, J. Beerten and X. Guillaud, "Application of Input Shaping Method to Vibrations Damping in a Type-IV Wind Turbine Interfaced with a Grid-Forming Converter," *Electric Power Systems Research*, vol. 210, p. 108083, 2022, https://doi.org/10.1016/j.epsr.2022.108083.

[14] S. Parman and H. Koguchi, "Rest-to-Rest Attitude Maneuvers of a Satellite with Flexible Solar Panels by using Input Shapers," *Computer Assisted Methods in Engineering and Science*, vol. 5, no. 4, pp. 421-441, 2023, https://cames.ippt.pan.pl/index.php/cames/article/view/1337.

[15] D. Lim, S. Hong, S. Ha, J. Kim and H. Lee, "Input-Shaping-based Improvement in the Machining Precision of Laser Micromachining Systems," *The International Journal of Advanced Manufacturing Technology*, vol. 125, pp. 4415-4424, 2023, https://doi.org/10.1007/s00170-023-10869-5.

[16] Y. Tang *et al.*, "Transient Acceleration Waveform Replication of Electro-Hydraulic Systems using Convex Combined Adaptive Controller with Input Shaping Technique," *ISA Transactions*, vol. 150, pp. 243-261, 2024, https://doi.org/10.1016/j.isatra.2024.05.012.

[17] L. Ramli, Z. Mohamed, A. M. Abdullahi, H. I. Jaafar and I. M. Lazim, "Control Strategies for Crane Systems: A Comprehensive Review," *Mechanical Systems and Signal Processing*, vol. 93, pp. 1-23, 2017, https://doi.org/10.1016/j.ymssp.2017.03.015.

[18] K. Hong and U. H. Shah, "Control Dynamics and Control of Industrial Cranes," *Springer Singapore*, 2019, https://doi.org/10.1007/978-981-13-5770-1.

[19] D. M. Munro, M. E. Govers and M. L. Oliver, "Physical Demands of Overhead Crane Operation," *International Journal of Industrial Ergonomics*, vol. 86, p. 103200, 2021, https://doi.org/10.1016/j.ergon.2021.103200.

[20] G. Kim, P. Pham, Q. H. Ngo and Q. C. Nguyen, "Neural Network-based Robust Anti-sway Control of an Industrial Crane Subjected to Hoisting Dynamics and Uncertain Hydrodynamic Forces," *International Journal of Control, Automation and Systems*, vol. 19, pp. 1953-1961, 2021, https://doi.org/10.1007/s12555-020-0333-9.

[21] N. Kayhani, H. Taghaddos, A. Mousaei, S. Behzadipour and U. Hermann, "Heavy Mobile Crane Lift Path Planning in Congested Modular Industrial Plants using a Robotics Approach," *Automation in Construction*, vol. 122, p. 103508, 2021, https://doi.org/10.1016/j.autcon.2020.103508.

[22] T. Gao, J. Huang and W. Singhose, "Eccentric-load Dynamics and Oscillation Control of Industrial Cranes Transporting Heterogeneous Loads," *Mechanism and Machine Theory*, vol. 172, p. 104800, 2022, https://doi.org/10.1016/j.mechmachtheory.2022.104800.

[23] Y. Man and Y. Liu, "Positioning and Antiswing Control of Overhead Crane Systems: A Supervisory Scheme," *Journal of the Franklin Institute*, vol. 360, no. 18, pp. 14329-14343, 2023, https://doi.org/10.1016/j.jfranklin.2023.10.038.

[24] C. Yang, J. Huang and W. Singhose, "Dynamic Modeling and Oscillation Control of Industrial Cranes Transporting Upright Slender Flexible Payloads," *Mechanical Systems and Signal Processing*, vol. 220, p. 111676, 2024, https://doi.org/10.1016/j.ymssp.2024.111676.

[25] K. Alghanim, A. Mohammed and M. T. Andani, "An Input Shaping Control Scheme with Application on Overhead Cranes," *International Journal of Nonlinear Sciences and Numerical Simulation*, vol. 20, no. 5, pp. 561-573, 2019, https://doi.org/10.1515/ijnsns-2018-0152.

[26] A. A. Fadli and E. Khorsid, "A Smooth Optimized Input Shaping Method for Two-Dimensional Crane Systems using Bezier Curves," *Transactions of the Institute of Measurement and Control*, vol. 43, no. 11, pp. 2512-2524, 2021, https://doi.org/10.1177/0142331221995305.

[27] S. M. F. U. Rehman, Z. Mohamed, A. R. Husain, H. I. Jaafar, M. H. Shaheed and M. A. Abbasi, "Input Shaping with an Adaptive Scheme for Swing Control of an Underactuated Tower Crane under Payload Hoisting and Mass Variations," *Mechanical Systems and Signal Processing*, vol. 175, p. 109106, 2022, https://doi.org/10.1016/j.ymssp.2022.109106.

[28] W. Tang, R. Ma, W. Wang and H. Gao, "Optimization-Based Input-Shaping Swing Control of Overhead Cranes," *Applied Sciences*, vol. 13, no. 17, p. 9637, 2023, https://doi.org/10.3390/app13179637.

[29] M. M. Bello, Z. Mohamed, S. M. F. U. Rehman, W. A. Balogun, K. Aibek and S. Gamzat, "Multi-Mode Input Shapers for Oscillation Control of an Overhead Crane with Distributed Mass Payload," *Applications of Modelling and Simulation*, vol. 8, pp. 191-200, 2024, http://arqiipubl.com/ojs/index.php/AMS_Journal/article/view/730.

[30] H. I. Jaafar, Z. Mohamed, M. A. Ahmad, N. A. Wahab, L. Ramli and M. H. Shaheed, "Control of an Underactuated Double-Pendulum Overhead Crane using Improved Model Reference Command Shaping: Design, Simulation and Experiment," *Mechanical Systems and Signal Processing*, vol. 151, p. 107358, 2021, https://doi.org/10.1016/j.ymssp.2020.107358.

[31] Y. Wu, N. Sun, H. Chen and Y. Fang, "New Adaptive Dynamic Output Feedback Control of Double-Pendulum Ship-Mounted Cranes With Accurate Gravitational Compensation and Constrained Inputs," *IEEE Transactions on Industrial Electronics*, vol. 69, no. 9, pp. 9196-9205, 2022, https://doi.org/10.1109/TIE.2021.3112978.

[32] G. Rigatos, "Nonlinear Optimal Control for the Underactuated Double-Pendulum Overhead Crane," *Journal of Vibration Engineering & Technologies*, vol. 12, pp. 1203-1223, 2024, https://doi.org/10.1007/s42417-023-00902-y.

[33] M. Lie, X. Wu, Y. Zhao and F. Li, "Output feedback control for overhead cranes subject to double-pendulum swing effects and uncertain disturbances," *Transactions of the Institute of Measurement and Control*, vol. 46, no. 7, pp. 1350-1361, 2024, https://doi.org/10.1177/01423312231196945.

[34] M. O. Elhabib, H. Wahid, Z. Mohamed and H. I. Jaafar, "Optimal Control of Double Pendulum Crane using FOPID and Genetic Algorithm," *Methods and Applications for Modeling and Simulation of Complex Systems*, vol. 1912, pp. 408-420, 2024, https://doi.org/10.1007/978-981-99-7243-2_34.

[35] M. M. Bello, Z. Mohamed, M. O. Efe and H. Ishak, "Modelling and Dynamic Characterisation of a Double-Pendulum Overhead Crane Carrying a Distributed-Mass Payload," *Simulation Modelling Practice and Theory*, vol. 134, p. 102953, 2024, https://doi.org/10.1016/j.simpat.2024.102953.

[36] M. R. Mojallizadeh, B. Brogliato and C. Prieur, "Modeling and Control of Overhead Cranes: A Tutorial Overview and Perspectives," *Annual Reviews in Control*, vol. 56, p. 100877, 2023, https://doi.org/10.1016/j.arcontrol.2023.03.002.

[37] Y. Zhao, X. Wu, F. Li and Y. Zhang, "Positioning and Swing Elimination Control of the Overhead Crane System with Double-Pendulum Dynamics," *Journal of Vibration Engineering & Technologies*, vol. 12, pp. 971-978, 2024, https://doi.org/10.1007/s42417-023-00887-8.

[38] S. Wang, W. Jin and W. Chen, "A Novel Payload Swing Control method based on Active Disturbance Rejection Control for 3D Overhead Crane Systems with Time-Varying Rope Length," *Journal of the Franklin Institute*, vol. 361, no. 6, p. 106707, 2024, https://doi.org/10.1016/j.jfranklin.2024.106707.

[39] N. Suksabai and I. Chuckpaiwong, "The Novel Design of the Command Smoother for Sway Suppression of Industrial Overhead Crane Considering Acceleration and Deceleration Limits," *International Journal of Dynamics and Control*, vol. 11, pp. 2082-2100, 2023, https://doi.org/10.1007/s40435-023-01156-y.

[40] Q. Zhang, B. Fan, L. Wang and Z. Liao, "Fuzzy Sliding Mode Control on Positioning and Anti-swing for Overhead Crane," *International Journal of Precision Engineering and Manufacturing*, vol. 24, pp. 1381-1390, 2023, https://doi.org/10.1007/s12541-023-00828-1.

[41] T. D. Kim, T. Nguyen, D. M. Do and H. X. Le, "Adaptive Neural Network Hierarchical Sliding Mode Control for Six Degrees of Freedom Overhead Crane," *Asian Journal of Control*, vol. 25, no. 4, pp. 2736-2751, 2023, https://doi.org/10.1002/asjc.2961.

[42] N. Suksabai and I. Chuckpaiwong, "Input-Shaped Model Reference Control using Sliding Mode Design for Sway Suppression of an Industrial Overhead Crane," *Engineering Journal*, vol. 27, no. 2, pp. 1-15, 2023, https://doi.org/10.4186/ej.2023.27.2.1.

[43] X. Cui, K. Chipusu, M. A. Ashraf, M. Riaz and J. Xiahou, "Symmetry-Enhanced LSTM-Based Recurrent Neural Network for Oscillation Minimization of Overhead Crane Systems during Material Transportation," *Symmetry*, vol. 16, no. 7, p. 920, 2024, https://doi.org/10.3390/sym16070920.

[44] W. Tang, E. Zhao, L. Sun and H. Gao, "An Active Swing Suppression Control Scheme of Overhead Cranes based on Input Shaping Model Predictive Control," *Systems Science & Control Engineering: An Open Access Journal*, vol. 11, no. 1, p. 2188401, 2023, https://doi.org/10.1080/21642583.2023.2188401.

[45] M. Alfares and K. Alhazza, "Comparative Analysis on the Performance of Different Types of Input-and Command-Shaping Controllers in Minimizing Payload Residual Vibration of an Overhead Crane with an Inclined Supporting Track," *International Journal of Mechanical System Dynamics*, vol. 4, no. 1, pp. 22–33, 2024, https://doi.org/10.1002/msd2.12095.

[46] S. Arabasi and Z. Masoud, "Frequency-Modulation Input-Shaping Strategy for Double-Pendulum Overhead Cranes Undergoing Simultaneous Hoist and Travel Maneuvers," *IEEE Access*, vol. 10, pp. 44954-44963, 2022, https://doi.org/10.1109/ACCESS.2022.3170099.

[47] Y. Huang, H. Li, J. Zhou and L. Meng, "Extra-Insensitive Shaper with Distributed Delays: Design and Vibration Suppress Analysis," *Journal of Vibration and Control*, vol. 26, no. 15-16, pp. 1185-1196, 2020, https://doi.org/10.1177/1077546319894490.

[48] M. A. Majeed, M. Alali, K. Alghanim and A. Alfadhli, "Integrated Time-Optimal Rigid-Body and Zero-Vibration Shapers on a Two Degrees of Freedom Overhead Crane System," *Journal of Vibration and Control*, 2024, https://doi.org/10.1177/10775463241257743.

[49] Y. Du, C. Wang, J. Lu and Y. Zhou, "Vibration Suppression using Multi-Impulse Robust Shaping Method of Zero Vibration and Derivative," *Journal of Sound and Vibration*, vol. 440, pp. 277-290, 2019, https://doi.org/10.1016/j.jsv.2018.10.038.

[50] B. Xu, R. Wang, B. Peng, F. A. Alqurashi and M. Salama, "Automatic Parameter Selection ZVD Shaping Algorithm for Crane Vibration Suppression based on Particle Swarm Optimisation," *Applied Mathematics and Nonlinear Sciences*, vol. 7, no. 1, pp. 73-82, 2022, https://doi.org/10.2478/amns.2021.1.00075.

[51] C. Kang, R. Hassan and K. Kim, "Analysis of a Generalized ZVD Shaper Using Impulse Vectors," *International Journal of Control, Automation and Systems*, vol. 18, pp. 2088–2094, 2020, https://doi.org/10.1007/s12555-019-0214-2.

[52] B. Lu, Y. Fang and N. Sun, "Enhanced-Coupling Adaptive Control for Double-Pendulum Overhead Cranes with Payload Hoisting and Lowering," *Automatica*, vol. 101, pp. 241–251, 2019, https://doi.org/10.1016/j.automatica.2018.12.009.

[53] L. Ramli, Z. Mohamed, M. O. Efe, I. M. Lazim and H. I. Jaafar, "Efficient Swing Control of an Overhead Crane with Simultaneous Payload Hoisting and External Disturbances," *Automation in Construction*, vol. 135, p. 106326, 2020, https://doi.org/10.1016/j.ymssp.2019.106326.

[54] W. Zhang, H. Chen, X. Yao and D. Li, "Adaptive Tracking of Double Pendulum Crane with Payload Hoisting/Lowering," *Automation in Construction*, vol. 141, p. 104368, 2022, https://doi.org/10.1016/j.autcon.2022.104368.

[55] M. Li, H. Chen and Z. Li, "Input-Limited Optimal Control for Overhead Cranes with Payload Hoisting/Lowering and Double Pendulum Effects," *Nonlinear Dynamics*, vol. 111, pp. 11135-11151, 2023, https://doi.org/10.1007/s11071-023-08420-y.

[56] M. J. Maghsoudi, L. Ramli, S. Sudin, Z. Mohamed, A. R. Husain and H. Wahid, "Improved Unity Magnitude Input Shaping Scheme for Sway Control of an Underactuated 3D Overhead Crane with Hoisting," *Mechanical Systems and Signal Processing*, vol. 123, pp. 466-482, 2019, https://doi.org/10.1016/j.ymssp.2018.12.056.

[57] A. M. Abdullahi, Z. Mohamed, H. Selamat, H. R. Pota, M. S. Z. Abidin and S. M. Fasih, "Efficient Control of a 3D Overhead Crane with Simultaneous Payload Hoisting and Wind Disturbance: Design, Simulation and Experiment," *Mechanical Systems and Signal Processing*, vol. 145, p. 106893, 2020, https://doi.org/10.1016/j.ymssp.2020.106893.

[58] C. Li, Q. Qi, Q. Dong, Y. Yu and Y. Fan, "Research on Fatigue Remaining Life of Structures for a Dynamic Lifting Process of a Bridge Crane," *Journal of Mechanical Science and Technology*, vol. 37, pp. 1789-1801, 2023, https://doi.org/10.1007/s12206-023-0319-7.

[59] Y. Wang, T. Yang, M. Zhai, Y. Fang and N. Sun, "Ship-Mounted Cranes Hoisting Underwater Payloads: Transportation Control With Guaranteed Constraints on Overshoots and Swing," *IEEE Transactions on Industrial Informatics*, vol. 19, no. 10, pp. 9968-9978, 2023, https://doi.org/10.1109/TII.2022.3230706.

[60] H. F. Karasu and M. Demirsoy, "Corrosion Cracking Resistance of Hoisting Ropes," *Materials Testing*, vol. 66, no. 3, pp. 347-358, 2024, https://doi.org/10.1515/mt-2023-0219.